Eur. Phys. J. E (2018) **41**: 46
DOI 10.1140/epje/i2018-11648-1

THE EUROPEAN PHYSICAL JOURNAL E

Regular Article

Jurin's law revisited: Exact meniscus shape and column height

Sai Liu, Shanpeng Li, and Jianlin Liu[a]

Department of Engineering Mechanics, College of Pipeline and Civil Engineering, China University of Petroleum (East China), Qingdao 266580, China

Received 5 February 2018 and Received in final form 7 March 2018
Published online: 30 March 2018 –

Abstract. Capillary rise of a liquid column is a historical problem, which has normally been formulated by Jurin's law. In the present study, we investigate the exact solutions of the column height, considering the real shape of the meniscus according to the Young-Laplace equation. The analytical solution in the planar model and the numerical solution in the axisymmetric model on the meniscus shape are both given, which are compared with the results from Jurin's law, modified Jurin's law and Surface Evolver simulation. The results quantitatively show that when the distance between the two plates or the diameter of the tube becomes bigger, Jurin's law and modified Jurin's law would cause serious errors, and the profile morphology of the meniscus must be calculated according to the Young-Laplace equation. These findings are beneficial for us to better understand the mechanism of capillarity and wetting, which are promising for such areas as oil displacement, ore floatation, building materials, fabrics, etc.

1 Introduction

Capillary action is the ability of a liquid flowing in narrow spaces without the assistance of, or even in opposition to, external forces like gravity. Capillary phenomena exist ubiquitously in the world, in a wide spectrum from our daily life to industrial and agricultural areas, such as water transportation in plants, water suction of soil, wetting of clothes and fabrics, ink injection of fountain pens, Kleenex's water absorbent ability, oil and gas displacement in rocks, and blood flowing in capillaries of human bodies [1,2]. Capillarity also plays a crucial role in some other aspects, such as the pearl droplets on lotus leaves [3], water strider walking on water surfaces [4], and shorebirds capturing food in use of their racket-like beak [5]. In these processes, the roughness of the solid surface can be modeled as capillary tubes or pillars, where the traditional Wenzel [6] and Cassie-Baxter models [7] have been adopted to predict the wetting behaviors.

The simplest example is the liquid column rise in a capillary tube, which has aroused great attention among many scholars, see Leonardo da Vinci, Robert Boyle, Jacob Bernoulli, Francis Hauksbee, Thomas Young, Pierre Simon Laplace, Friedrich Gauss, Lord Kelvin, and Albert Einstein. Among others, the most celebrated work is the famous Jurin's law, which says that the height of the rising column in a capillary tube is inversely proportional to the tube diameter [8]. Another pioneering work worthwhile mentioning is the famous Young-Laplace equation [9], which is used to formulate the meniscus shape in the front of the column. Yet the derivation of Jurin's law is not trivial, as there are several approaches to get it. The first one is based on the hydrostatic pressure and the Young-Laplace equation, the second one on the force balance, and the third one on the energy principle; and there are many debates to discuss the equivalence of the deduction of Jurin's law [10–15]. Recently, Rodriguez-Valverde and Miranda stressed that the aforementioned two ways of hydrostatic pressure and mechanics are equivalent [16], and Barozzi and Angeli derived the law by minimizing the free energy of the whole system [17]. However, when the solid wall is viewed as a soft material, its deformation would be coupled with the capillary rise. A number of works have been carried out on this issue, and it is pointed out that the height of the column between two elastic sheets must be modified [18–20]. In addition, the dynamics behavior of the capillary rise has also become a hot topic in the past decades, and the most important landmark is just the Lucas-Washburn equation [21, 22]. In succession, many following works were focused on the modification of this equation, including the considered factors as energy dissipation, inertial effect, low Reynolds number, liquid-vapor coupling, etc. [23–26].

Although much effort has been made on the capillarity phenomenon, there is still a lack of quantitative analysis to judge, when to use Jurin's law and to what extent Jurin's law applies. Up to now, the reports on this problem are rarely seen, and the reason may be ascribed to the strong nonlinearity of the governing equation of the meniscus, and thus seeking its analytical solution is an intractable

[a] e-mail: liujianlin@upc.edu.cn (corresponding author)

task. As a big challenge, we try to solve the nonlinear equation of the meniscus in the planar model and axisymmetric model, by using analytical and numerical skills.

The outline of this paper is organized as follows. In sect. 2, we look back at the classical Jurin's law, and give the expression of the modified Jurin's law. In sect. 3, we consider the two-dimensional model on the capillarity, and derive the analytical solutions of the profile shape and critical parameters on the meniscus. In sect. 4, according to the Young-Laplace equation, we numerically solved the meniscus morphology and related parameters in the axisymmetric model. In sect. 5, we analyze the effects of Young's contact angle and distance parameter on the meniscus shape and column height. Although we only consider both the planar model and axisymmetric model on the capillary rise, the simulation scheme is also adaptable to the meniscus with any shape. It is noted that the real surface of the tube is, to a certain degree, not chemically or geometrically homogeneous, which would cause the contact angle hysteresis [27,28]. However, for this elementary model in conventional mechanics, the contact angle hysteresis is not considered, *i.e.* we only take Young's contact angle in calculation.

2 Classical Jurin's law

We first retrospect the capillary rise of a liquid column confined between two parallel plates, or within a capillary tube vertically inserted into the liquid reservoir, which is schematized in fig. 1. The distance between the two plates, or the diameter of the capillary tube, is denoted by the variable d. If the solid wall is hydrophilic, a liquid column always rises between the two plates or inside the tube wall, whose height from the liquid level to the triple contact line (TCL) is denoted by H. Normally, two assumptions are made here: The first one is that the meniscus shape is considered as part of a circle or a spherical surface for these two cases; and the second one is that, the volume of the liquid between the TCL and the level corresponding to the lowest point of the meniscus is ignored. These two cases are referred to as the two-dimensional or planar model and the axisymmetric model, respectively.

Based upon the above two assumptions, and according to the force balance, one can get the value of the column height

$$H = \frac{2\gamma \cos\theta_{\mathrm{Y}}}{\rho g d} \tag{1}$$

for the two-dimensional case, and

$$H = \frac{4\gamma \cos\theta_{\mathrm{Y}}}{\rho g d} \tag{2}$$

for the axisymmetric case. In eqs. (1) and (2), the symbol γ is the surface tension of the liquid, ρ the density of the liquid, g the gravitational acceleration, and θ_{Y} the Young's contact angle of the solid wall. Equations (1) and (2) are the so-called Jurin's laws, which are the widely used and most traditional models to predict the column height.

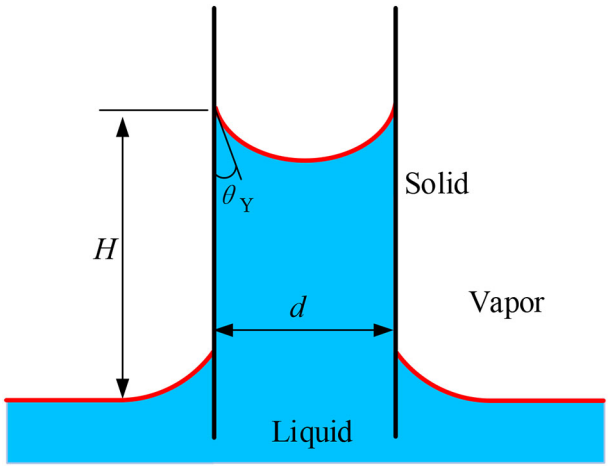

Fig. 1. Schematic of the capillary rise, where a liquid column is confined within two parallel solid walls or a capillary tube.

If we want to get a more rigorous model, then it is postulated that the meniscus still satisfies the first assumption, but the ignored mass of the meniscus should be compensated. Henceforth, the height of the liquid column would be modified to

$$H_{\mathrm{M}} = H + \frac{d}{8\cos^2\theta_{\mathrm{Y}}}\left(\pi - 2\theta_{\mathrm{Y}} - \sin 2\theta_{\mathrm{Y}}\right) \tag{3}$$

for the planar model. Similarly, the modified height of the liquid column in the axisymmetric model is written as

$$H_{\mathrm{M}} = H + \frac{d}{6\cos^3\theta_{\mathrm{Y}}}\left(2 - 3\sin\theta_{\mathrm{Y}} + \sin^3\theta_{\mathrm{Y}}\right). \tag{4}$$

From our qualitative estimation, it can be judged that when the distance or diameter d is sufficiently small, the above-mentioned assumptions do not lead to great errors. However, when the distance becomes bigger, it will cause serious problems to predict the critical parameters during capillary rise. For the latter case, the key point lies in that the real morphology of the meniscus cannot be well depicted by the circular or spherical geometry, and its profile shape must satisfy the Young-Laplace equation; and thus a detailed analysis must be performed. Due to this reason, the two above assumptions must be abandoned in what follows.

3 Planar model

As a typical case study, let us consider the two-dimensional or the planar meniscus arising between a vertical wall and the water level, and only one half of the meniscus is selected due to its symmetry. Refer to the Cartesian coordinate system O-xz as shown in fig. 2. The height of the TCL is represented as h as shown in the figure. According to the geometric configuration, the boundary conditions are given as

$$\begin{aligned} &x = 0, \qquad z = h, \qquad z' = -\cot\theta_{\mathrm{Y}}; \\ &x = d/2, \qquad z = 0, \qquad z' = 0, \end{aligned} \tag{5}$$

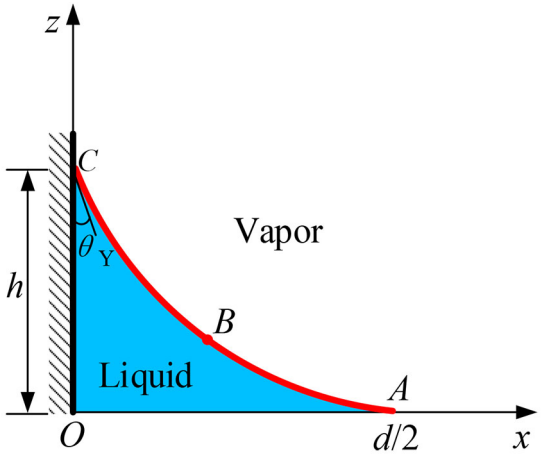

Fig. 2. Schematic of the meniscus profile in the planar model, which spans between a solid wall and the liquid level.

where the prime over a variable stands for its derivative with respect to x.

Assume the atmospheric pressure to be p_0, and at the lowest point of the meniscus, *i.e.* point A, one has

$$p_A = p_0 - \Delta p_A, \tag{6}$$

where p_A is the pressure at point A inside the liquid-vapor interface, and Δp_A is the over pressure across this interface. In line with the Young-Laplace equation, the Laplace pressure difference is expressed as

$$\Delta p_A = \gamma c_0, \tag{7}$$

where c_0 is the curvature at point A.

The pressure at an arbitrary point B on the meniscus profile is written as

$$p_B = p_A - \rho g z. \tag{8}$$

Inserting eqs. (6) and (7) into (8) leads to the Laplace pressure difference at point B

$$\Delta p_B = p_0 - p_B = \gamma c_0 + \rho g z. \tag{9}$$

Therefore, at point B, the Young-Laplace equation yields

$$\frac{z''}{[1+(z')^2]^{3/2}} = c_0 + \frac{\rho g z}{\gamma}, \tag{10}$$

where the left term of eq. (10) represents the curvature at point B in the Cartesian coordinate system. It should be mentioned that the governing equation of the two-dimensional meniscus shape has the same format as that of a planar beam in large deformation, which is termed as "elastica" [29]. Although this equation is strongly nonlinear, its analytical solution can be obtained at hand.

Define the capillary length $\kappa^{-1} = \sqrt{\gamma/(\rho g)}$ and let $\kappa^2 t = c_0 + \kappa^2 z$, and then eq. (10) is recast as

$$\frac{t''}{[1+(t')^2]^{3/2}} = \kappa^2 t. \tag{11}$$

Multiplying t' to both sides of eq. (11) and integrating from both sides of the equation, one can get

$$\frac{1}{\sqrt{1+(t')^2}} = -\frac{\kappa^2}{2}t^2 + C, \tag{12}$$

where C is an integration constant.

The boundary conditions are then transformed to

$$\begin{aligned} &x = 0, \qquad t = h + \kappa^{-2} c_0, \qquad t' = z' = -\cot\theta_{\mathrm{Y}}; \\ &x = d/2, \qquad t = \kappa^{-2} c_0, \qquad t' = z' = 0. \end{aligned} \tag{13}$$

Substituting the boundary conditions in eq. (13) into eq. (12), the integration constant and the TCL height can be determined as

$$C = 1 + c_0^2 \kappa^{-2}/2, \tag{14}$$

$$h = \kappa^{-1}\sqrt{2(C - \sin\theta_{\mathrm{Y}})} - \kappa^{-2} c_0. \tag{15}$$

Let $2C - \kappa^2 t^2 = 2\sin\phi$ and insert it into eq. (12), and the following integration can be reached:

$$\int_{d/2}^{x} \mathrm{d}x = \int_{\pi/2}^{\phi} \frac{\sqrt{2}}{2}\kappa^{-1}\frac{\sin\phi}{\sqrt{C-\sin\phi}}\mathrm{d}\phi. \tag{16}$$

We also introduce the transformation relation $1+\sin\phi = 2k^2\sin^2\theta = (1+C)\sin^2\theta$, where $C = 2k^2 - 1$, and $\mathrm{d}\phi = \frac{2k\cos\theta}{\sqrt{1-k^2\sin^2\theta}}\mathrm{d}\theta$. Consequently, the horizontal coordinate of an arbitrary point on the meniscus profile can be expressed in terms of the elliptic integrals of the first and second kinds:

$$x = d/2 + \kappa^{-1}\int_{\theta_0}^{\theta}\left(\frac{1}{\sqrt{1-k^2\sin^2\theta}} - 2\sqrt{1-k^2\sin^2\theta}\right)\mathrm{d}\theta, \tag{17}$$

where $\cos\theta_0 = \kappa^{-1}c_0/(2k)$. Especially at point C, we have the relation

$$0 = \frac{d}{2} + \kappa^{-1}\int_{\theta_0}^{\theta_h}\left(\frac{1}{\sqrt{1-k^2\sin^2\theta}} - 2\sqrt{1-k^2\sin^2\theta}\right)\mathrm{d}\theta, \tag{18}$$

where $\cos\theta_h = (\kappa h + \kappa^{-1}c_0)/(2k)$. Based on eq. (18), one can build the correlation between the distance d and the curvature at point A, *i.e.* the variable c_0.

In the light of the relation $2C - \kappa^2 z^2 = 2\sin\phi$, one can get the vertical coordinate at an arbitrary point on the meniscus profile

$$z = \sqrt{2}\kappa^{-1}\sqrt{1 + C - 2k^2\sin^2\theta} - \kappa^{-2}c_0. \tag{19}$$

Similarly, when the solid wall is hydrophobic, *i.e.* Young's contact angle $\theta_{\mathrm{Y}} > 90°$, the related formulas for the meniscus profile's shape and the TCL height are further deduced as

$$h = -\kappa^{-1}\sqrt{2(C - \sin\theta_{\mathrm{Y}})} - \kappa^{-2}c_0, \tag{20}$$

$$z = \sqrt{2}\kappa^{-1}\sqrt{1 + C - 2k^2\sin^2\theta} - \kappa^{-2}c_0 \tag{21}$$

$$x = d/2 + \kappa^{-1}\int_{\theta_0}^{\theta}\left(2\sqrt{1-k^2\sin^2\theta} - \frac{1}{\sqrt{1-k^2\sin^2\theta}}\right)\mathrm{d}\theta. \tag{22}$$

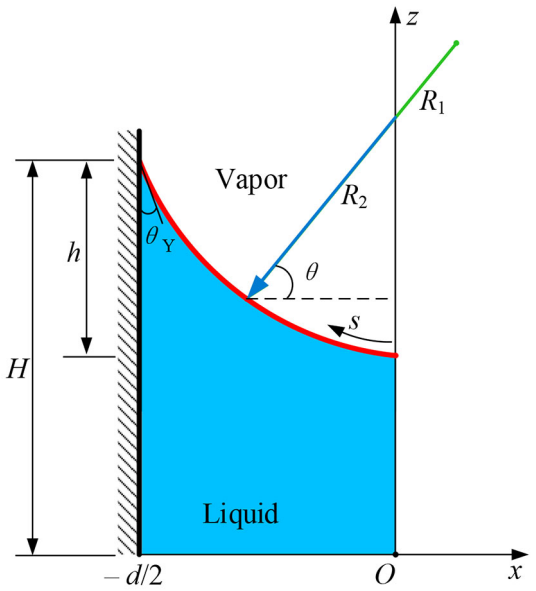

Fig. 3. Schematic of meniscus profile in the axisymmetric tube, where a quarter of the meniscus is selected due to the symmetry.

Moreover, for both the hydrophilic and hydrophobic solid surfaces, the column height can be derived as

$$H = \kappa^{-2} c_0 + h. \tag{23}$$

4 Axisymmetric model

Next we consider the axisymmetric model, *i.e.* the climbing of a liquid column across the inside wall of a capillary tube. Refer to the Cartesian coordinate system O-xz for the meniscus profile as shown in fig. 3. Then the boundary conditions are formulated as

$$\begin{aligned} &x = -d/2, \qquad z' = -\cot\theta_{\mathrm{Y}}; \\ &x = 0, \qquad z' = 0. \end{aligned} \tag{24}$$

Let R_1 and R_2 be the two principal radii at any point on the meniscus profile, and then we have the following geometric relations:

$$\mathrm{d}s = R_1 \mathrm{d}\theta, \tag{25}$$

$$R_2 \cos\theta = -x, \tag{26}$$

where the symbol s is the arc length along the meniscus profile in the xz-plane, θ is the angle between the radius R_2 and the horizontal line.

The summation of $1/R_1$ and $1/R_2$ is defined as the average curvature, which is related with the pressure difference across the liquid-vapor interface via the Young-Laplace equation:

$$\frac{\mathrm{d}\theta}{\mathrm{d}s} + \frac{\cos\theta}{-x} = \kappa^2 z, \tag{27}$$

i.e.

$$\frac{z''}{[1+(z')^2]^{3/2}} + \frac{z'}{x[1+(z')^2]^{1/2}} = \kappa^2 z \tag{28}$$

in the Cartesian coordinate system, where eqs. (25) and (26) are inserted.

Evidently, there is no analytical solution on the second-order differential equation (28) in combination with the boundary conditions (24). Therefore, a numerical method, *i.e.* the shooting method, is adopted, and a self-developed Matlab program is developed to solve the equation.

5 Results and discussion

By analyzing the above governing equation and formulas, the meniscus shape, TCL height and column height can all be determined by two kernel parameters, *i.e.* Young's contact angle θ_{Y}, and the distance or diameter d.

5.1 Meniscus shape

The curves of the meniscus profile in the planar case or axisymmetric configuration can be depicted in figs. 4 and 5, respectively, where (a) $d = 1\,\mathrm{mm}$, $\theta_{\mathrm{Y}} = 30°$; (b) $d = 20\,\mathrm{mm}$, $\theta_{\mathrm{Y}} = 30°$; (c) $d = 1\,\mathrm{mm}$, $\theta_{\mathrm{Y}} = 120°$; (d) $d = 20\,\mathrm{mm}$, $\theta_{\mathrm{Y}} = 120°$. For these two cases, all of the curves reveal consistent trends, and there are some common features to be clarified.

The first one is that, when the solid wall is hydrophilic, *i.e.* Young's contact angle θ_{Y} is smaller than 90°, the meniscus arises above the level, as shown in fig. 4(a), (b) and fig. 5(a), (b); and vice versa, the meniscus sinks below the level, as shown in fig. 4(c), (d) and fig. 5(c), (d). The neutral case is that when Young's contact angle $\theta_{\mathrm{Y}} = 90°$, and the meniscus is always a horizontal line according to the analytical solution in the planar case, *i.e.* eqs. (17) and (19). In the axisymmetric model, when $\theta_{\mathrm{Y}} = 90°$, the boundary conditions would degenerate into $z' = 0$ at $x = 0$ and $x = -d/2$, and thus the differential equation with two point boundaries must have a zero solution, that is the horizontal surface of the meniscus.

Next, the TCL height h is also dependent upon Young's contact angle. For Jurin's law based on the circle and spherical cap assumptions, the expression of TCL height $h = d(1 - \sin\theta_{\mathrm{Y}})/(2\cos\theta_{\mathrm{Y}})$. If $\theta_{\mathrm{Y}} < 90°$, the value of h is bigger than 0; and if $\theta_{\mathrm{Y}} > 90°$, the value of h is smaller than 0. Our analytical solution in the planar case and the numerical solution in the axisymmetric model obey the same law. Especially, in the planar case, when $\theta_{\mathrm{Y}} = 90°$, the expression of the TCL height $h = \kappa^{-1}\sqrt{2(C-1)} - \kappa^{-2} c_0 = 0$. Since the numerical solution for the meniscus shape is always zero when $\theta_{\mathrm{Y}} = 90°$, thus the TCL height h is also zero in the axisymmetric case. In order to get a better comparison on the results of meniscus shape and TCL height, we also conduct the numerical simulation in use of the free software Surface Evolver [30]. From figs. 4 and 5, we can see that the four results, *i.e.*, those based on Jurin's law, modified Jurin's law,

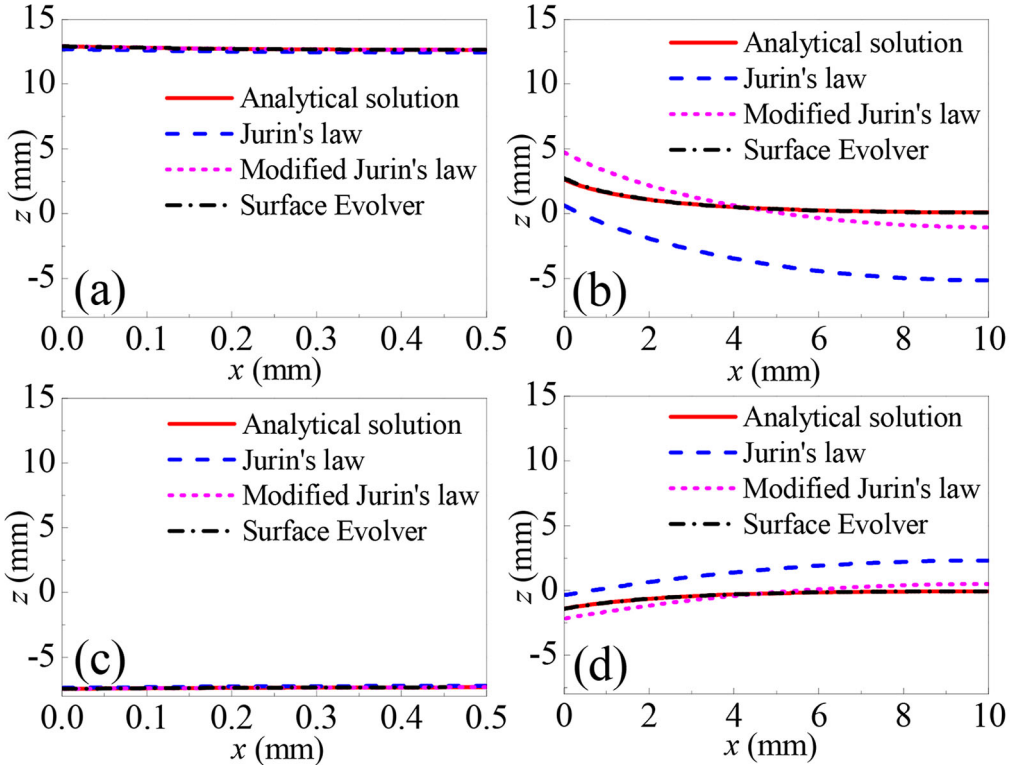

Fig. 4. Calculated meniscus profile in the planar model, where (a) $d = 1\,\text{mm}$, $\theta_\text{Y} = 30°$; (b) $d = 20\,\text{mm}$, $\theta_\text{Y} = 30°$; (c) $d = 1\,\text{mm}$, $\theta_\text{Y} = 120°$; (d) $d = 20\,\text{mm}$, $\theta_\text{Y} = 120°$.

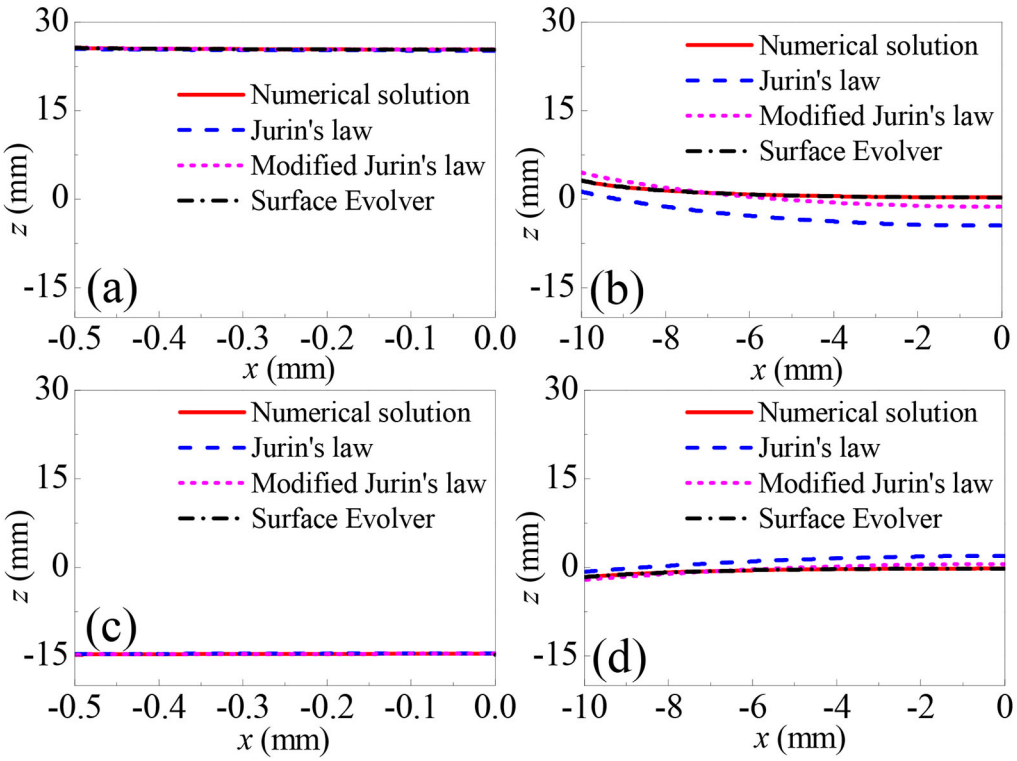

Fig. 5. Calculated meniscus profile in the axisymmetric model, where (a) $d = 1\,\text{mm}$, $\theta_\text{Y} = 30°$; (b) $d = 20\,\text{mm}$, $\theta_\text{Y} = 30°$; (c) $d = 1\,\text{mm}$, $\theta_\text{Y} = 120°$; (d) $d = 20\,\text{mm}$, $\theta_\text{Y} = 120°$.

our analytical or numerical solution and Surface Evolver simulation all abide by the same laws.

Then we consider the influence of another parameter, *i.e.* the distance or diameter d. Obviously, whether Young's contact angle $\theta_Y < 90°$ or $\theta_Y > 90°$, when the value of d is small enough, such as $d = 1\,\text{mm}$, the four curves are nearly overlapped, which are shown in fig. 4(a), (c) and fig. 5(a), (c). In this case, the liquid volume occupied by the meniscus is negligible compared with the whole liquid column, thus the modified Jurin's law does not differ from Jurin's law, and they are also very close to our analytical or numerical solutions and the Surface Evolver simulation. In this case, the circular or spherical assumption on the meniscus profile can be perfectly accepted. However, when the value of d becomes much bigger, such as $d = 20\,\text{mm}$, there are great differences among Jurin's law, modified Jurin's law, and our results, which are displayed in fig. 4(b), (d) and fig. 5(b), (d). In this situation, the Surface Evolver simulation is also in excellent agreement with our analytical and numerical solutions, but these results strongly deviate from those of Jurin's law and modified Jurin's law. Therefore, for the big value of the distance or diameter d, the classical assumptions on the circular or spherical shape of the meniscus profile, and the ignorance of the liquid volume occupied by the meniscus cannot be adopted, as they would cause serious errors in practice.

Similarly, whenever Young's contact angle $\theta_Y < 90°$ or $\theta_Y > 90°$, the height value of the TCL h is proportional to the parameter d according to its expression based on Jurin's law. This law has been validated by our analytical or numerical solutions when the parameter d is small, which is shown in fig. 4(a), (c) and fig. 5(a), (c). However, there are big deviations among Jurin's law, modified Jurin's law, and our calculated results, which are shown in fig. 4(b), (d) and fig. 5(b), (d). For instance, in the planar case, there are big differences, *i.e.* around several millimeters on the TCL height from these results. We also find that if the distance or diameter d is big enough, the TCL height does not change, attaining to a limit value. This fact stresses that when the solid walls are too far away, they would not affect each other, thus the meniscus near the boundary would keep its stable shape with a more increase of d.

5.2 Column height

It should also be mentioned that, the fact that the TCL height h increases with the increase of the parameter d may cause an illusion, *i.e.* the "capillary effect" is more significant when d becomes bigger. Then a puzzled question is raised: how to characterize the capillary effect properly? This emerging question is directed towards inspecting another parameter, *i.e.* the height of the liquid column, instead of the height of the TCL.

The dependence relationships between the column height H and the parameter d in the planar model and axisymmetric model are shown in figs. 6 and 7, respectively, where Young's contact angle is taken as 30°. It is

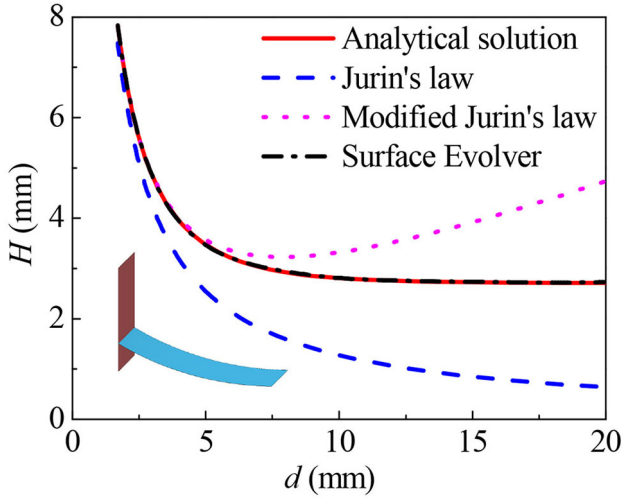

Fig. 6. Column height with respect to the distance d in the planar model, where $\theta_Y = 30°$.

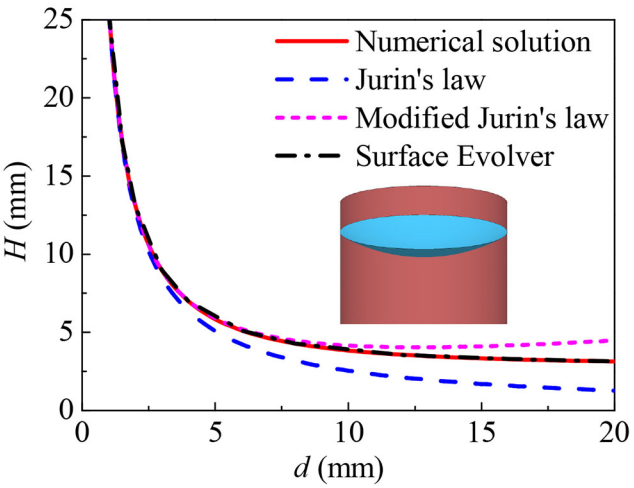

Fig. 7. Column height with respect to the diameter d in the axisymmetric model, where $\theta_Y = 30°$.

clearly seen that, if the parameter d is sufficiently small, *i.e.* below 1 mm, the results from Jurin's law and modified Jurin's law match our calculated results very well. However, there exist big differences among these results when the parameter d becomes bigger, but our analytical or numerical result is still in consistence with the Surface Evolver simulation. In this case the curves from the modified Jurin's law demonstrate nonmonotonic behaviors, and this phenomenon is due to the fact that in this model the circle or spherical cap assumption on the meniscus profile is considered, yet this assumption does not apply any more with the increase of d. Besides this feature, it can be seen that the modified Jurin's law has a higher precision and a broader applicable range than the classical one, which is shown in figs. 6 and 7.

Furthermore, it can be found from figs. 6 and 7 that, the column height H decreases with the increase of the parameter d, and this rule is opposite to that of the TCL height h. The daily experience tells us that when the

parameter d becomes smaller, the capillary effect would be more obvious. This fact may remind us that to appropriately characterize the capillary effect, the column height should be selected, instead of the TCL height.

6 Conclusions

In conclusion, we make an extensive investigation on the capillary rise of a liquid column confined between two parallel plates or within a capillary tube. The analytical solutions of the meniscus shape and column height in the two-dimensional case are derived in terms of elliptic integrals. Then we numerically solved the Young-Laplace equation which depicts the meniscus profile in the axisymmetric model, and the meniscus and related parameters are computed.

The effects of Young's contact angle and the distance parameter d on the meniscus shape and column height are fully analyzed. The results show that, if the solid wall is hydrophilic, the meniscus would climb over the water level; and vice versa, it would sink below the level. When the distance parameter is small, such as within the capillary length, the meniscus shape and column height can be well predicted by Jurin's law and modified Jurin's law, which are in excellent agreement with the results from our analytical and numerical calculations. However, if the distance parameter exceeds the capillary length, great differences would occur among these four models, *i.e.* Jurin's law, modified Jurin's law, analytical or numerical solution and Surface Evolver simulation. We also point out that the column height instead of the TCL height should be used to characterize the capillary effect.

Although only the planar model and axisymmetric model on the capillary rise are considered, the proposed analysis approach, including the numerical simulation can be extended to the meniscus with an arbitrary shape. These findings are beneficial for us to better understand the mechanism of capillarity and wetting, which hold great implications in such areas as oil displacement, ore floatation, building materials, fabrics, etc.

This project was supported by the National Natural Science Foundation of China (11672335), Key Research and Development Project in Shandong Province (2017GGX20117), and the Fundamental Research Funds for the Central Universities of China (17CX06018).

Author contribution statement

Jianlin Liu made the formulation of the model, and wrote the paper. Sai Liu and Shanpeng Li conducted the calculations and simulations.

References

1. D. Quéré, Physica A **313**, 32 (2002).
2. R. Blossey, Nat. Mater. **2**, 301 (2003).
3. W. Barthlott, C. Neinhuis, Planta **202**, 1 (1997).
4. D.L. Hu, B. Chan, J.W. Bush, Nature **424**, 663 (2004).
5. M. Prakash, D. Quéré, J.W.M. Bush, Science **320**, 931 (2008).
6. R.N. Wenzel, Ind. Eng. Chem. **28**, 988 (1936).
7. A.B.D. Cassie, S. Baxter, Trans. Faraday Soc. **40**, 546 (1944).
8. J. Jurin, Philos. Trans. R. Soc. Lond. **30**, 739 (1718).
9. T. Young, Philos. Trans. R. Soc. Lond. **95**, 65 (1805).
10. E.K. Chapin, Am. J. Phys. **27**, 617 (1959).
11. J.B.T. McCaughan, Phys. Educ. **22**, 100 (1987).
12. J.B.T. McCaughan, Phys. Educ. **23**, 205 (1988).
13. G.C. Vorlicek, J.W. Warren, G.E. Kilby, Phys. Educ. **23**, 7 (1988).
14. P.O. Scheie, Am. J. Phys. **57**, 279 (1989).
15. J.B.T. McCaughan, Am. J. Phys. **60**, 87 (1992).
16. M.A. Rodriguez-Valverde, M.T. Miranda, Eur. J. Phys. **32**, 49 (2011).
17. G.S. Barozzi, D. Angeli, Energy Proc. **45**, 548 (2014).
18. H.Y. Kim, L. Mahadevan, J. Fluid Mech. **548**, 141 (2006).
19. J. Bico, B. Roman, L. Moulin, A. Boudaoud, Nature **432**, 690 (2004).
20. J.L. Liu, X.Q. Feng, R. Xia, H.P. Zhao, J. Phys. D: Appl. Phys. **40**, 5564 (2007).
21. R. Lucas, Kolloidn. Zh. **23**, 15 (1918).
22. E.W. Washburn, Phys. Rev. **17**, 273 (1921).
23. E. Brittin, J. Wesley, Appl. Phys. **17**, 37 (1946).
24. J. Szekely, A.W. Neumann, Y.K Chuang, J. Colloid Interface Sci. **35**, 273 (1971).
25. S. Levine, P. Reed, E.J. Watson, G. Neale, in *Colloid and Interface Science* (Academic Press, 1976) pp. 403–419.
26. F. Maggi, F. Alonso-Marroquin, Int. J. Multiphase Flow **42**, 62 (2012).
27. E. Bormashenko, Colloid Polym. Sci. **291**, 339 (2013).
28. G. Whyman, E. Bormashenko, T. Stein, Chem. Phys. Lett. **450**, 355 (2008).
29. J.L. Liu, Chin. Phys. Lett. **26**, 116803 (2009).
30. K.A. Brakke, Exp. Math. **1**, 141 (1992).